Theoretical and Experimental Study of the ^{13}C Chemical Shift Tensors of Acetone Complexed with Brønsted and Lewis Acids

Dewey H. Barich,[†] John B. Nicholas,*[,‡] Teng Xu,[†] and James F. Haw*[,†]

Contribution from The Center for Catalysis, Department of Chemistry, Texas A&M University, P.O. Box 300012, College Station, Texas 77842-3012, and Environmental Molecular Sciences Laboratory, Pacific Northwest National Laboratory, Richland, Washington 99352

Received June 25, 1998

Abstract: We calculated the chemical shift tensors for acetone and 12 complexes of acetone with Brønsted and Lewis acids. Each complex was optimized at the MP2/6-311+G* or B3LYP/DZVP2 level of theory. Chemical shift tensors were calculated with the gauge including atomic orbital (GIAO) approach at the RHF and MP2 levels of theory. We discovered a strong correlation between the MP2 and RHF ^{13}C isotropic shifts of the carbonyl carbon in the complexes studied. Linear regression indicates that the MP2 isotropic shifts can be predicted by $\delta_{MP2} = [1.12\ (\pm 0.04)]\delta_{RHF} - 42.1\ (\pm 10.5)$ ppm ($R^2 = 0.9974$). We were thus able to study two systems that are currently intractable at the GIAO-MP2 level. One is the complex of acetone with a large model of a zeolite, $(H_3SiO)_3SiOHAl(OSiH_3)_3$. The RHF shift of the carbonyl carbon of acetone on the zeolite model (238.4 ppm) is in poor agreement with the experimental (223 ppm) value. However, the MP2 result predicted by the linear correlation (224.0 ppm) is in much closer agreement. We were also able to study acetone adsorbed on aluminum chloride powder models. We find that acetone·$AlCl_3$ is a poor adsorption model, as demonstrated by a large discrepancy between experimental and calculated MP2 shifts. However, the MP2 shift from the regression equation (244.7 ppm) for acetone complexed to the larger Al_2Cl_6 cluster is in excellent agreement with the experimental result (245 ppm). We also report experimental measurements of the principal components of the carbonyl ^{13}C shift tensor for a variety of solid acids, including frozen oleum and frozen SbF_5.

Introduction

The ^{13}C isotropic chemical shift of carbonyl groups in ketones and aldehydes is strongly sensitive to the interaction of the carbonyl oxygen with Brønsted and Lewis acids. In Brønsted acids, the shift reflects the extent of proton transfer to the carbonyl group.[1,2] For example, acetone has an isotropic chemical shift of 206.0 ppm in $CDCl_3$[3] whereas it is 250 ppm in superacid solutions,[4] in which acetone is completely protonated. The large change in chemical shift due to protonation is qualitatively explained by the hydroxycarbenium resonance structure, which places a partial positive charge on the carbonyl carbon:

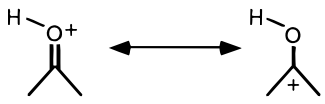

Significant chemical shift changes are also observed for aldehydes and ketones interacting with strong Lewis sites. For example, an isotropic shift of 245 ppm was reported for acetone-*2*-^{13}C complexed to aluminum chloride.[5] This result may also be explained by a positively charged carbon. The shifts of ketones and aldehydes in acidic media are increasingly being interpreted in a quantitative manner. For example, Farcasiu has developed acidity functions from the ^{13}C shifts of mesityl oxide (4-methyl-3-penten-2-one) and 4-hexen-3-one and used them to characterize the strengths of various liquid acids.[6,7]

Ketones and aldehydes also show large ^{13}C isotropic shift changes on solid Brønsted acids such as zeolites. The relative magnitudes of the observed changes generally agree with other rankings of relative acid strength. Although acidity functions cannot be applied to solid acids with the thermodynamic rigor of solution measurements, it is still insightful to compare the ^{13}C shift of a given molecule on a solid acid with liquid acids that produce the same isotropic shift. For example, two of us synthesized mesityl oxide in zeolites by the dimerization of acetone followed by dehydration.[8] The ^{13}C shifts we measured in the zeolites were in the range of those measured by Farcasiu in 60−80% H_2SO_4. Acetone has been widely applied as a probe molecule for Brønsted sites in zeolites.[8−11] Significant changes in chemical shifts can also be induced by complexation to Lewis

* To whom correspondence should be addressed.
[†] Texas A&M University.
[‡] Pacific Northwest National Laboratory.

(1) Maciel, G. E.; Ruben, G. C. *J. Am. Chem. Soc.* **1963**, *85*, 3903−3904.
(2) Maciel, G. E.; Natterstad, J. J. *J. Chem. Phys.* **1965**, *42*, 2752−2759.
(3) Hawkes, G. E.; Herwig, K.; Roberts, J. D. *J. Org. Chem.* **1974**, *39*, 1017.
(4) Olah, G. A.; White, A. M. *J. Am. Chem. Soc.* **1969**, *91*, 5801.
(5) Xu, T.; Torres, P. D.; Beck, L. W.; Haw, J. F. *J. Am. Chem. Soc.* **1995**, *117*, 8027−8028.
(6) Farcasiu, D.; Ghenciu, A.; Miller, G. J. *J. Catal.* **1992**, *134*, 118−125.
(7) Farcasiu, D.; Ghenciu, A. *J. Am. Chem. Soc.* **1993**, *115*, 10901−10908.
(8) Xu, T.; Munson, E. J.; Haw, J. F. *J. Am. Chem. Soc.* **1994**, *116*, 1962−1972.
(9) Bosácek, V. *J. Phys. Chem.* **1993**, *97*, 10732−10737.
(10) Biaglow, A. I.; Sepa, J.; Gorte, R. J.; White, D. *J. Catal.* **1995**, *151*, 373−384.
(11) Haw, J. F.; Xu, T.; Nicholas, J. B.; Goguen, P. W. *Nature* **1997**, *389*, 832−835.

10.1021/ja982226w CCC: $15.00
Published on Web 11/12/1998

sites in metal-exchanged zeolites.[5] Other ketones and aldehydes that have been studied in zeolites by NMR include cyclopentanone, diacetone alcohol, acetophenone, acetaldehyde, crotonaldehyde, benzaldehyde, and propionaldehyde.[8,12−15]

The interpretation of NMR chemical shifts is being revolutionized by theoretical developments. A variety of methods are now available for the calculation of NMR data. These methods include the individual gauge localized orbitals (IGLO),[16,17] local orbital local origin (LORG),[18,19] and the gauge including atomic orbitals (GIAO) approaches.[20,21] While lack of electron correlation was an issue in the past, density functional theory (DFT) implementations of all these methods have become available.[22−25]

To achieve meaningful agreement with experimental values, adequate basis sets and sufficient treatment of electron correlation must be used, both in obtaining the optimized geometry and in the NMR calculation itself. Although NMR calculations at the RHF level often give reasonable results, many molecules require inclusion of electron correlation in order to achieve agreement with experiment. While computationally expedient, GIAO-DFT methods currently available for chemical shift calculations can give appreciable errors, as the GIAO-DFT method did for the benzenium cation.[25] In contrast, the GIAO-MP2 method of Gauss[26] was repeatedly proven[27−29] to have high accuracy, even for demanding cases such as carbenium ions. We recently reported very good agreement between experimental and theoretical ^{13}C isotropic shifts and satisfactory agreement for principal components for a variety of carbenium ions including the isopropyl cation,[30] acylium cations,[28] and simple alkylbenzenium cations[29] on solid superacidic media. Unfortunately, GIAO-MP2 calculations are computationally much more expensive than GIAO-RHF or GIAO-DFT calculations with the same basis set. In addition, the GIAO-MP2 implementation in ACES II[31] is limited to 300 basis functions. Even reaching that limit generally requires use of symmetry. Considering that the systems under study theoretically must reasonably represent the chemistry observed experimentally, we often require models that are too large for us to treat with the GIAO-MP2 method. Indeed, the need to treat such large systems is the primary motivation for this work.

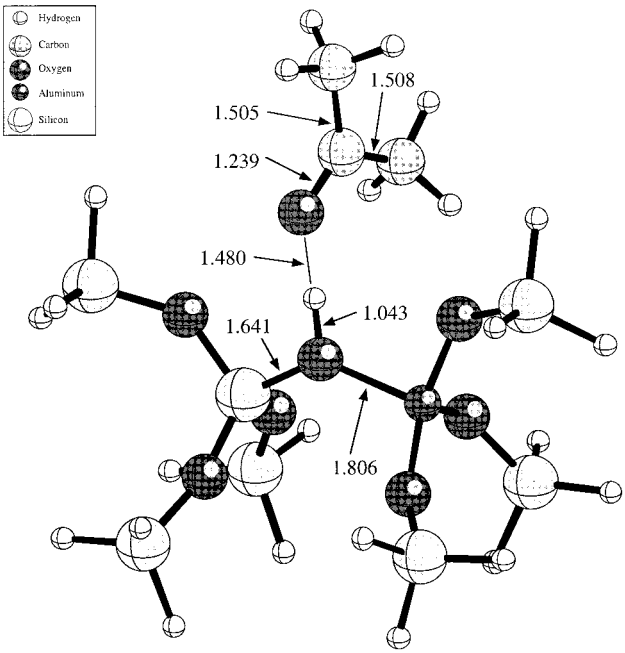

Figure 1. B3LYP/DZVP2 optimized structure of acetone hydrogen-bonded to a zeolite cluster model of zeolite HZSM-5. Selected bond distances (Å) are shown.

One such system we wanted to study was the complex that acetone forms with Brønsted acid sites in zeolites. Typical aldehydes and ketones form hydrogen-bonded complexes with acid sites in zeolites in which the proton either remains on the lattice or is intermediate between the lattice and the carbonyl oxygen.[32] The interatomic distances in these systems are typical of strong hydrogen bonds. A fundamental understanding of hydrogen bonding between zeolite acid sites and aldehydes and ketones, and the associated effect on ^{13}C chemical shift tensors, would greatly contribute to the interpretation of spectral changes observed in Brønsted acid media. Unfortunately, our prior experience indicates that accurate calculation of the acetone•zeolite complex requires a zeolite model such as $(H_3SiO)_3SiOHAl(OSiH_3)_3$ (seen with acetone in Figure 1), which is much too large to treat with the GIAO-MP2 method and adequate basis sets with ACES II. Even the acetone complex with the minimal $H_3SiOHAlH_3$ model pushes the limits of the GIAO-MP2 approach when a sufficiently large basis set is employed.

Another interesting complex is that of acetone and the Lewis acid aluminum chloride. As we will show, $AlCl_3$ is a poor model of acetone adsorption on aluminum chloride powder. However, acetone complexed to an Al_2Cl_6 model of the surface gives quantitative agreement with experiment. As in the acetone zeolite case, we found the complex with the larger Al_2Cl_6 model to be too large to study at the GIAO-MP2 level with an adequate basis set.

We were able to overcome this problem when we discovered a high correlation between the calculated GIAO-RHF and GIAO-MP2 carbonyl carbon isotropic chemical shifts for a variety of complexes of acetone with small Brønsted and Lewis acids. With the use of linear regression, we are now able to make accurate predictions of the GIAO-MP2 chemical shifts of large systems from the GIAO-RHF values. For acetone

(12) Zhang, J.; Krawietz, T. R.; Skloss, T. W.; Haw, J. F. *J. Chem. Soc., Chem. Commun.* **1997**, 685−686.
(13) Munson, E. J.; Haw, J. F. *Angew. Chem.* **1993**, *105*, 643−646.
(14) Xu, T.; Zhang, J.; Haw, J. F. *J. Am. Chem. Soc.* **1995**, *117*, 3171−3178.
(15) Xu, T.; Zhang, J.; Munson, E. J.; Haw, J. F. *J. Chem. Soc., Chem. Commun.* **1994**, 2733−2735.
(16) Kutzelnigg, W. *Isr. J. Chem.* **1980**, *19*, 193−200.
(17) Schindler, M.; Kutzelnigg, W. *J. Chem. Phys.* **1982**, *76*, 1919−1933.
(18) Hansen, A. E.; Bouman, T. D. *J. Chem. Phys.* **1985**, *82*, 5035−5047.
(19) Hansen, A. E.; Bouman, T. D. *J. Chem. Phys.* **1989**, *91*, 3552−3560.
(20) Ditchfield, R. *Mol. Phys.* **1974**, *27*, 789−807.
(21) Wolinski, K.; Hinton, J. F.; Pulay, P. *J. Am. Chem. Soc.* **1990**, *112*, 8251−8260.
(22) Malkin, V. G.; Malkina, O. L.; Casida, M. E.; Salahub, D. R. *J. Am. Chem. Soc.* **1994**, *116*, 5898−5908.
(23) Schreckenbach, G.; Ziegler, T. *J. Phys. Chem.* **1995**, *99*, 606−611.
(24) Arduengo, J. A.; Dixon, D. A.; Kumashiro, K. K.; Lee, C.; Power, W. P.; Zilm, K. W. *J. Am. Chem. Soc.* **1994**, *116*, 6361−6367.
(25) Cheeseman, J. R.; Trucks, G. W.; Keith, T. A.; Frisch, M. J. *J. Chem. Phys.* **1996**, *104*, 5497−5509.
(26) Gauss, J. *Chem. Phys. Lett.* **1992**, *191*, 614−620.
(27) Sieber, S.; Schleyer, P. v. R.; Gauss, J. *J. Am. Chem. Soc.* **1993**, *115*, 6987−6988.
(28) Xu, T.; Torres, P. D.; Barich, D. H.; Nicholas, J. B.; Haw, J. F. *J. Am. Chem. Soc.* **1997**, *119*, 396−405.
(29) Xu, T.; Barich, D. H.; Torres, P. D.; Haw, J. F. *J. Am. Chem. Soc.* **1997**, *119*, 406−414.
(30) Nicholas, J. B.; Xu, T.; Barich, D. H.; Torres, P. D.; Haw, J. F. *J. Am. Chem. Soc.* **1996**, *118*, 4202−4203.
(31) Stanton, J. F.; Gauss, J.; Watts, J. D.; Lauderdale, W. J.; Bartlett, R. J. *Int. J. Quantum Chem.* **1992**, *S26*, 879−894.
(32) Haw, J. F.; Nicholas, J. B.; Xu, T.; Beck, L. W.; Ferguson, D. B. *Acc. Chem. Res.* **1996**, *29*, 259−267.

adsorption on both the zeolite and aluminum chloride models, the GIAO-MP2 carbonyl chemical shifts *predicted* by the regression equation are in excellent agreement with experimental values, whereas the *calculated* GIAO-RHF values are substantially different.

We also report experimental work carried out for acetone on various solid acids. Principal components of the ^{13}C chemical shift tensors of acetone-*2*-^{13}C were measured at low temperature for frozen neat acetone, acetone in zeolite HZSM-5, acetone in frozen oleum (30% SO_3/H_2SO_4), and acetone adsorbed on a number of metal salt powders.

Theoretical Methods

The molecules and complexes studied include acetone, the acetone dimer, protonated acetone, adducts of acetone with HF, HCl, CH_3OH, H_2F_2, 2 HF, BF_3, AlF_3, $AlCl_3$, and Al_2Cl_6. Finally, we investigated the complex of acetone with a large zeolite model, $(H_3SiO)_3SiOHAl(OSiH_3)_3$. The geometries of most of these molecules and complexes were optimized with second-order Møller−Plesset perturbation theory[33] (MP2) and the 6-311+G* basis set.[34] Acetone complexed with Al_2Cl_6 was optimized at the MP2/6-311++G** level. The core electrons were frozen in all MP2 optimizations. Acetone complexed with the $(H_3SiO)_3SiOHAl(OSiH_3)_3$ zeolite model was optimized with density functional theory at the B3LYP[35] level and the DZVP2[36] basis set. An MP2/6-311+G* optimization of the zeolite complex would be extremely expensive, if not intractable, with currently available hardware and software. We have found the B3LYP/DZVP2 level of theory to give geometries very similar to MP2/6-311+G*. Only the central 10 atoms ($O_3SiOHAlO_3$) of the zeolite model were allowed to move, whereas the peripheral atoms were held in crystallographic positions of the T(12)−O(24)−T(12) site in HZSM-5.[37] Frequency calculations were performed at MP2/6-311+G* for most of the species presented here. All optimizations and frequencies were performed with Gaussian 94.[38] Chemical shieldings were calculated with the GIAO method at the RHF and MP2 levels with the program ACES II[31] with the exception of the acetone·zeolite and acetone·Al_2Cl_6 complexes. The number of basis functions required for these complexes was larger than ACES II can accept. We thus obtained GIAO-RHF NMR data for these complexes with Gaussian 94. We used Ahlrichs'[39] qzp {611111/4111/1} for the C and O in the carbonyls, tzp {51111/311/1} on the other heavy atoms, and dz {31} on the hydrogens in the chemical shift calculations. All chemical shift calculations used six Cartesian d orbitals. In addition to the qzp/tzp/dz chemical shift calculations, we also calculated chemical shifts with tzp for all heavy atoms. For simplicity we refer to the qzp/tzp/dz and tzp/dz basis set schemes as qzp and tzp, respectively.

The calculated chemical shielding tensors were symmetrized and then diagonalized in order to yield principal components.[28] These were then referenced to the ^{13}C isotropic chemical shift of carbon in tetramethylsilane (TMS) calculated at the same level of theory (for both the shielding and geometry) such that $\delta_{calc} = \sigma_{TMS} - \sigma_{calc}$. The absolute shieldings of ^{13}C in TMS are reported in Table 1.

Table 1. GIAO-RHF and GIAO-MP2 ^{13}C Calculated Isotropic Chemical Shifts of TMS (ppm)

optimization level	basis[a]	RHF	MP2
MP2/6-311+G*	qzp/tzp/dz	193.4	198.6
MP2/6-311+G*	tzp/dz	193.2	199.0
MP2/6-311++G**	qzp/tzp/dz	193.2	198.4[b]
MP2/6-311++G**	tzp/dz	193.0	198.8[b]
B3LYP/DZVP2	qzp/tzp/dz	192.8	198.1[b]
B3LYP/DZVP2	tzp/dz	192.6	198.4[b]

[a] Basis set scheme used in the chemical shift calculations. [b] Value included for completeness; not used in this study.

The isotropic chemical shift is the average of the principal components, which are defined such that $\delta_{11} \geq \delta_{22} \geq \delta_{33}$. Thus

$$\delta_{iso} = {}^1/_3(\delta_{11} + \delta_{22} + \delta_{33})$$

The asymmetry factor (η) and chemical shift anisotropy (CSA) are defined by the following equations as found in a compilation of chemical shift anisotropy data:[40]

for $|\delta_{11} - \delta_{iso}| \geq |\delta_{33} - \delta_{iso}|$

$$CSA = {}^3/_2(\delta_{11} - \delta_{iso}) \quad (1a)$$

$$\eta = (\delta_{22} - \delta_{33})/(\delta_{11} - \delta_{iso}) \quad (1b)$$

for $|\delta_{11} - \delta_{iso}| \leq |\delta_{33} - \delta_{iso}|$

$$CSA = {}^3/_2(\delta_{33} - \delta_{iso}) \quad (1c)$$

$$\eta = (\delta_{22} - \delta_{11})/(\delta_{33} - \delta_{iso}) \quad (1d)$$

Experimental Methods

Materials. Magnesium chloride (98%), magnesium bromide (98%), zinc chloride (99.999%), zinc iodide (99.999%), aluminum chloride (99.99%), aluminum bromide (99.99+%), aluminum iodide (99.999%), tantalum(V) fluoride (98%), tantalum(V) chloride (99.99%), scandium(III) trifluoromethanesulfonate, antimony pentafluoride, 30% oleum (30% SO_3/H_2SO_4), and 1,1,1,3,3,3-hexafluoro-2-propanol (99.8+%) were obtained from Aldrich. Zeolite HZSM-5 was obtained from the UOP Corp. Acetone-*2*-^{13}C (99% ^{13}C enrichment) was obtained from Cambridge Isotope Co. All reagents were used without further purification.

Sample Preparation for MAS NMR. A standard CAVERN device[41−43] was used for the sample preparation throughout this investigation. A typical procedure for sample preparation was as follows. A 0.3−1.0 g sample of metal halide powder was loaded into a 7.5 mm zirconia rotor inside a drybox under a nitrogen atmosphere. The rotor was placed into the CAVERN device, attached to a vacuum line, and evacuated to a final pressure of less than 10^{-4} Torr. For liquid samples, several freeze−pump−thaw cycles were applied instead of evacuation at room temperature. Adsorptions were generally done at low temperatures.[44] The loading of acetone-*2*-^{13}C varied from experiment to experiment but was typically 0.2−0.5 mmol/g.

NMR Spectroscopy. ^{13}C NMR experiments were performed on a modified Chemagnetics CMX-300 spectrometer operating at 75.36 MHz. We used hexamethylbenzene (17.4 ppm for the methyl carbons) as the external chemical shift standard. Chemical shift parameters are reported relative to TMS. Chemagnetics-style pencil probes spun 7.5 mm zirconia rotors at 1−6.5 kHz with active spin speed control (±3 Hz).

Cross polarization[45] spectra were acquired at 77 K with a contact time of 2 ms, a pulse delay of 1−5 s, and 2000 transients. The principal

(33) Møller, C.; Plesset, M. S. *Phys. Rev.* **1934**, *46*, 618−622.
(34) Hehre, W. J.; Radom, L.; Schleyer, P. v. R.; Pople, J. A. *Ab Initio Molecular Orbital Theory*; John Wiley & Sons: New York, 1986.
(35) Becke, A. D. *J. Chem. Phys.* **1993**, *98*, 5648−5652.
(36) Godbout, N.; Salahub, D. R.; Andzelm, J.; Wimmer, E. *Can. J. Chem.* **1992**, *70*, 560−571.
(37) van Koningsveld, H.; van Bekkum, H.; Jansen, J. C. *Acta Crystallogr.* **1987**, *B43*, 127−132.
(38) Frisch, M. J.; Trucks, G. W.; Schlegal, H. B.; Gill, P. M. W.; Johnson, B. G.; Robb, M. A.; Cheeseman, J. R.; Keith, T.; Petersson, G. A.; Montgomery, J. A.; Raghavachari, K.; Al-Laham, M. A.; Zakrzewski, V. G.; Ortiz, J. V.; Foresman, J. B.; Cioslowski, J.; Stefanov, B. B.; Nanayakkara, A.; Challacombe, M.; Peng, C. Y.; Ayala, P. Y.; Chen, W.; Wong, M. W.; Andres, J. L.; Replogle, E. S.; Gomperts, R.; Martin, R. L.; Fox, D. J.; Binkley, J. S.; Defrees, D. J.; Baker, J.; Stewart, J. P.; Head-Gordon, M.; Gonzalez, C.; Pople, J. A. *Gaussian 94*, Revision B.2; Gaussian Inc.: Pittsburgh, PA, 1995.
(39) Schäfer, A.; Horn, H.; Ahlrichs, R. *J. Chem. Phys.* **1992**, *97*, 2571−2577.
(40) Duncan, T. M. *A Compilation of Chemical Shift Anisotropies*; Farragut Press: Chicago, IL, 1990.
(41) Munson, E. J.; Ferguson, D. B.; Kheir, A. A.; Haw, J. F. *J. Catal.* **1992**, *136*, 504−509.
(42) Munson, E. J.; Murray, D. K.; Haw, J. F. *J. Catal.* **1993**, *141*, 733−736.
(43) Xu, T.; Haw, J. F. *Top. Catal.* **1997**, *4*, 109−118.
(44) Haw, J. F.; Richardson, B. R.; Oshiro, I. S.; Lazo, N. L.; Speed, J. A. *J. Am. Chem. Soc.* **1989**, *111*, 2052−2058.

Table 2. Theoretical Gas-Phase Energies of Acetone and Complexes with Acetone (hartrees)

system	MP2 energy[a]	ZPE[b]	thermal[b]	total
acetone	−192.611 895	0.084 835	0.005 362	−192.521 698
acetone·acetone	−385.229 649	0.170 842	0.012 597	−385.046 210
acetone·$HOCH_3$	−308.030 513	0.138 914	0.010 136	−307.881 463
acetone·HCl	−652.851 235	0.093 777	0.008 181	−652.749 277
acetone·HF	−292.887 593	0.097 121	0.007 760	−292.782 712
acetone·H_2F_2	−393.163 206	0.109 649	0.010 025	−393.043 532
acetone·2HF	−393.160 881	0.109 696	0.010 226	−393.040 959
acetone·BF_3	−516.617 304	0.099 870	0.009 192	−516.508 242
acetone·AlF_3	−733.910 452	0.095 112	0.010 670	−733.804 670
acetone·$AlCl_3$	−1813.798 667	*c*	*c*	−1813.798 667
acetone·H^+	−192.918 109	0.097 933	0.005 324	−192.814 852

[a] Energy from the MP2/6-311+G* optimization. [b] ZPE and thermal energies calculated at MP2/6-311+G* on the MP2/6-311+G* optimized structure; frequency calculations performed at 1 atm and 298.15 K. [c] Due to computational expense, this frequency calculation was not attempted; thus this value was not determined.

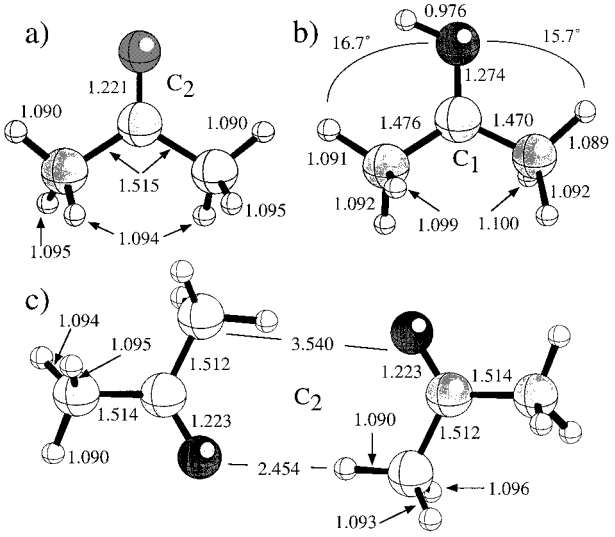

Figure 2. MP2/6-311+G* optimized structures of (a) acetone, (b) protonated acetone, and (c) the acetone dimer. Symmetry point group, selected bond distances (Å), and bond angles (eg) are shown.

components of the chemical shift tensors were extracted by fitting the sideband intensities of the ^{13}C CP MAS spectra with the Herzfeld−Berger algorithm.[46] The sample rotation speeds were set so as to provide at least 3 orders of spinning sidebands, and in most cases 5 orders of sidebands were acquired.

Theoretical Results

Structures Modeling Hydrogen Bonding and Protonation. Total energies for all of the structures reported here, including (in most cases) thermal corrections, are reported in Table 2. Calculated gas-phase structures of acetone, protonated acetone, and a hydrogen-bonded acetone dimer are reported in Figure 2. The internal coordinates for acetone in Figure 2 are consistent with those in earlier work[47] and in a recent report for acetone optimized at MP2/tzp;[48] and a frequency analysis shows that the minimum-energy geometry has C_2 symmetry. The calculated proton affinity of acetone at MP2/6-311+G* is 185.4 kcal/mol. The C−O bond distance is 1.221 Å and both C−C bond distances are 1.515 Å (cf. 1.220 and 1.514 Å at MP2/tzp[48]). This geometry is qualitatively similar to that of the isopropyl cation,[30,49] although the isopropyl cation had considerably stronger hyperconjugative interactions. An NBO analysis[50,51] of the acetone molecule here shows evidence of only very weak hyperconjugation between the π orbital of the carbonyl C and an antibonding σ^* orbital from a C−H bond of each methyl group. By symmetry, there are only three distinct hydrogens in the acetone molecule. The C−H bond distance involved in weak hyperconjugation is 1.095 Å (cf. 1.121 Å in the isopropyl cation).[30] The H−C−C−O dihedral angle is 113.6°; therefore, the C−H bond is 23.6° off the perpendicular to the heavy atom plane. The other C−H distances are 1.090 Å for the hydrogen nearest the heavy atom plane and 1.094 Å for the remaining bond.

Protonation increases the C−O bond distance of acetone by 0.053 Å. The C−C bond lengths have decreased by 0.039 and 0.045 Å, and the protons nearest the carbonyl plane have rotated to about 16° from that plane (cf. 6.7° in isolated acetone). While addition of the proton formally lowers symmetry to C_1, the methyl groups are essentially in C_2 symmetry.

The gas-phase dimer of acetone is also presented. The two molecules form a weak hydrogen bond (2.4 kcal/mol without a basis set superposition error correction), with each acting as both hydrogen bond donor and acceptor. The distance from the carbonyl O to the methyl H is 2.454 Å. The effects of weak hydrogen bonding are evident: the C−O bond length has increased slightly compared to that of the isolated molecule, and the C−C bond has decreased slightly as well.

In Figure 3a the gas-phase structure is shown for the complex between acetone and methanol. Methanol proves to be a weak proton donor to acetone in the gas phase. The O−O distance (2.892 Å) is characteristic of a weak hydrogen bond. The C−O bond distance in acetone increases very slightly from 1.221 to 1.226 Å upon complexation with methanol. The C−C distances are decreased slightly to 1.511 Å.

We next considered three different complexes formed between acetone and hydrogen fluoride. These are acetone complexed to a single HF molecule (acetone·HF), acetone complexed to an HF dimer (acetone·H_2F_2), and acetone complexed to two separate HF molecules (acetone·2HF) (Figure 3b−d). Formation of acetone·HF increased the C−O bond distance only 0.006 Å relative to the isolated acetone molecule. The C−C bond distance decreased by 0.006 Å for the methyl group nearest the HF and decreased by 0.008 Å for the other methyl

(45) Pines, A.; Gibby, M. G.; Waugh, J. S. *J. Chem. Phys.* **1973**, *59*, 569−590.
(46) Herzfeld, J.; Berger, A. E. *J. Chem. Phys.* **1980**, *73*, 6021−6030.
(47) Krivdin, L. B.; Zinchenko, S. V.; Kalabin, G. A.; Facelli, J. C.; Tufro, M. F.; Contreras, R. H.; Denisov, A. Y.; Gavrilyuk, O. A.; Mamatyuk, V. I. *J. Chem. Soc., Faraday Trans.* **1992**, *88*, 2459−2463.
(48) Gonzales, N.; Simons, J. *Int. J. Quantum Chem.* **1997**, *63*, 875−894.
(49) Koch, W.; Schleyer, P. v. R.; Buzek, P.; Liu, B. *Croat. Chem. Acta* **1992**, *65*, 655−672.
(50) Reed, A. E.; Curtiss, L. A.; Weinhold, F. *Chem. Rev.* **1988**, *88*, 899.
(51) Glendening, E. D.; Reed, A. E.; Carpenter, J. E.; Weinhold, F. *NBO*, Version 3.1.

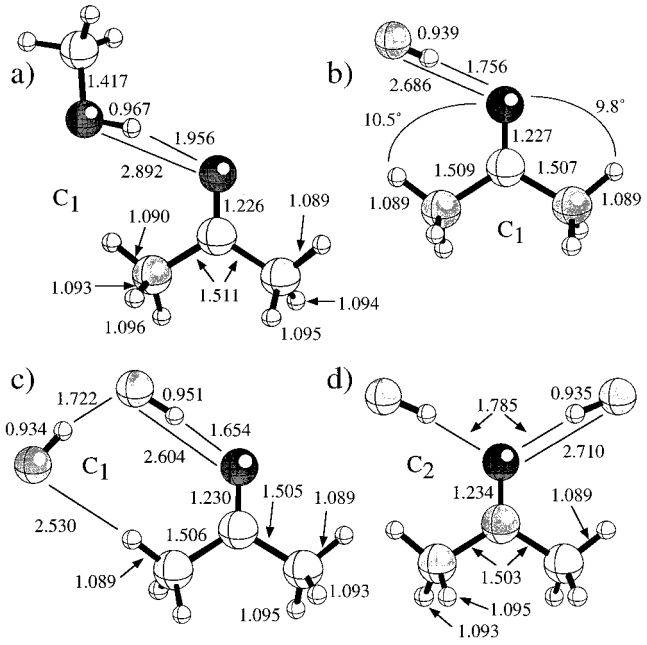

Figure 3. MP2/6-311+G* optimized structures of (a) acetone·CH_3OH, (b) acetone·HF, (c) acetone·H_2F_2, and (d) acetone·2HF. Symmetry point group, selected bond distances (Å), and bond angles (deg) are shown.

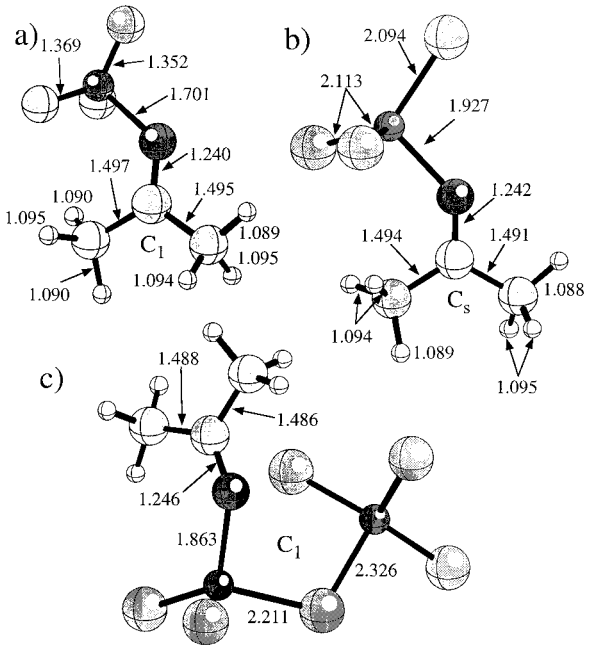

Figure 4. Optimized structures of (a) acetone·BF_3, (b) acetone·$AlCl_3$, and (c) acetone·Al_2Cl_6. Symmetry point group and selected bond distances (Å) are shown. (a) and (b) were optimized at MP2/6-311+G*, while (c) was optimized at MP2/6-311++G**.

group. The lowest energy complex of acetone and two HF molecules is acetone·H_2F_2. The C−O distance here is increased by 0.009 Å from isolated acetone, and the C−C distance has decreased by 0.009 Å (methyl nearest the H_2F_2) and 0.010 Å (methyl farthest from the H_2F_2). Acetone·2HF is 1.6 kcal/mol higher in energy than acetone·H_2F_2, including thermal corrections, and has a C−O distance of 1.234 Å. The C−C bonds here have decreased to 1.503 Å, a greater change than is found for acetone·H_2F_2. Acetone·HCl is qualitatively similar to acetone·HF but has a C−O distance of 1.226 Å and C−C bond lengths of 1.510 Å for the methyl carbon nearest the HCl and 1.509 Å for the other methyl carbon. Its geometry is provided in the Supporting Information.

The structure of acetone complexed to a model of zeolite HZSM-5 is reported in Figure 1. Upon formation of a complex with acetone, the zeolite Si−O bond length has decreased from 1.658 to 1.643 Å, the Al−O distance has also decreased from 1.826 to 1.808 Å, and the O−H bond has lengthened from 0.971 to 1.038 Å. The Si−O−Al angle has decreased from 130.8 to 127.0°. All these changes in geometry are consistent with proton donation from the zeolite to acetone.

Structures Modeling Coordination to Lewis Acids. Gas-phase structures of acetone·BF_3, acetone·$AlCl_3$, and acetone·Al_2Cl_6 are shown in Figure 4. For acetone·BF_3, the C−O bond distance has increased by 0.019 Å compared to that of isolated acetone and the C−C bonds have decreased by 0.018 Å (nearest the BF_3) and 0.020 Å (farthest from the BF_3). In the $AlCl_3$ complex, the C−O bond distance increases by 0.021 Å relative to free acetone, and for Al_2Cl_6, it increases by 0.025 Å. Note that, for the case of the acetone·Al_2Cl_6 complex, the optimized geometry of Al_2Cl_6 is quite different from the known D_{2h} geometry of the isolated dimer. The acetone O−Al distance is considerably shorter for the aluminum chloride dimer than for the monomer (1.863 Å vs 1.927 Å). The shortening of the O−Al distance is consistent with our expectation that the dimer is a much stronger Lewis acid than the monomer. The C−C bond distances have decreased by 0.021 Å (nearest the $AlCl_3$) and 0.024 Å (farthest from $AlCl_3$). For the complex of acetone with Al_2Cl_6, the C−C bond distances have decreased by 0.029 Å (nearest the acetone-coordinated Al atom) and 0.027 Å (farthest from the acetone-coordinated Al atom). The geometry of acetone·AlF_3 is provided in the Supporting Information. In acetone·AlF_3, the C−O distance is 0.021 Å longer than that in isolated acetone and the C−C bond distances have decreased by 0.020 Å (nearest the AlF_3) and 0.024 Å (farthest from the AlF_3) upon complexation with the Lewis acid.

Chemical Shift Calculations. Calculated ^{13}C chemical shift data for acetone and the complexes of acetone in Figures 1−4 obtained at GIAO-RHF/qzp and (in most cases) also at GIAO-MP2/qzp are reported in Table 3. Also included in Table 3 are chemical shifts calculated at GIAO-RHF/tzp and GIAO-MP2/tzp. The GIAO-MP2/tzp scheme has performed very well for several challenging systems. Here this scheme did very well with respect to trends, but we found that better agreement with experimental values was obtained by treating both atoms in the carbonyl group with a qzp basis set. For example, the experimental gas-phase chemical shift of acetone is 201.2 ppm.[52] At the GIAO-MP2/tzp level of theory, we calculated a value of 197.0 ppm. In contrast, the GIAO-MP2/qzp chemical shift of 202.8 ppm is in closer agreement with experiment. Therefore, in the following, we primarily focus on the shifts calculated with the qzp/tzp/dz basis set scheme.

Protonation in the gas phase has a dramatic effect on the ^{13}C isotropic chemical shift of acetone. At GIAO-MP2/qzp, the isotropic chemical shift increases from 202.8 to 260.1 ppm in the protonated molecule. All other structures considered had theoretical shifts within this range. The GIAO-MP2/qzp shift is sensitive to even the weakest complex formation; the acetone dimer shifts to 207.3 ppm. We did not attempt to explicitly model acetone in solution, but for comparison, the literature value for $CDCl_3$ is 206.0 ppm.[3] Partial proton transfer results in intermediate protonation shifts; for example, acetone·H_2F_2 is shifted to 217.9 ppm.

(52) Jameson, A. K.; Jameson, C. J. *Chem. Phys. Lett.* **1987**, *134*, 461−466.

Table 3. ^{13}C Calculated Chemical Shift Data for Acetone and Models of Acetone Interacting with a Variety of Brønsted and Lewis Acids

	MP2/qzp/tzp/dz						RHF/qzp/tzp/dz					
system	δ_{iso}, ppm	δ_{11}, ppm	δ_{22}, ppm	δ_{33}, ppm	CSA, ppm	η	δ_{iso}, ppm	δ_{11}, ppm	δ_{22}, ppm	δ_{33}, ppm	CSA, ppm	η
acetone	202.8	281	237	90	−169	0.39	217.5	323	254	75	−214	0.49
acetone·acetone	207.3	282	249	91	−174	0.29	222.0	323	267	75	−220	0.38
acetone·$HOCH_3$	210.7	283	259	89	−182	0.20	224.6	322	277	75	−224	0.30
acetone·HCl	211.4	282	263	89	−183	0.16	225.7	321	282	74	−227	0.26
acetone·HF	213.4	284	268	88	−188	0.13	227.7	321	288	73	−231	0.22
acetone·H_2F_2	217.9	288	277	88	−195	0.08	231.0	319	300	74	−236	0.12
acetone·2HF	223.3	297	286	87	−204	0.08	236.7	319	319	72	−246	0.00
acetone·BF_3	228.8	326	276	83	−218	0.34	243.1	354	305	70	−260	0.28
acetone·$AlCl_3$	236.8	349	275	86	−226	0.50	248.7	376	298	72	−265	0.44
acetone·AlF_3	238.3	348	281	86	−229	0.43	249.8	373	304	71	−268	0.39
acetone·H^+	260.1	416	282	83	−265	0.76	267.9	442	291	70	−296	0.76
acetone·zeolite	225.6[a] 224.0[b]						238.4	326	317	73	−249	0.05
acetone·Al_2Cl_6	244.7[a] 243.1[b]						255.4	405	290	71	−277	0.62

	MP2/tzp/dz						RHF/tzp/dz					
system	δ_{iso}, ppm	δ_{11}, ppm	δ_{22}, ppm	δ_{33}, ppm	CSA, ppm	η	δ_{iso}, ppm	δ_{11}, ppm	δ_{22}, ppm	δ_{33}, ppm	CSA, ppm	η
acetone	197.0	274	228	88	−163	0.42	211.9	317	246	72	−210	0.51
acetone·acetone	201.7	276	240	89	−169	0.32	216.5	317	260	72	−216	0.40
acetone·$HOCH_3$	205.3	277	251	87	−177	0.23	219.7	317	271	71	−222	0.32
acetone·HCl	206.0	276	254	87	−178	0.19	220.4	316	274	71	−224	0.28
acetone·HF	208.1	278	260	86	−183	0.15	222.4	316	281	70	−228	0.23
acetone·H_2F_2	212.5	282	270	86	−190	0.10	226.3	315	294	70	−234	0.14
acetone·2HF	218.0	289	280	85	−199	0.06	231.4	314	311	70	−243	0.01
acetone·BF_3	224.5	321	272	81	−215	0.34	238.5	348	301	66	−258	0.28
acetone·$AlCl_3$	232.6	343	271	84	−223	0.49	244.3	370	294	69	−263	0.44
acetone·AlF_3	233.9	341	277	83	−226	0.42	245.2	367	300	68	−266	0.38
acetone·H^+	255.0	407	278	80	−262	0.74	262.9	434	288	67	−294	0.75
acetone·zeolite	220.6[c] 224.8[b]						233.5	320	311	69	−246	0.06
acetone·Al_2Cl_6	240.5[c] 244.7[b]						251.1	399	286	68	−275	0.62

[a] Estimated from the GIAO MP2/qzp vs RHF/qzp correlation described in the text. [b] Value for predicted δ_{iso} when referenced to gas-phase acetone (see text for details). [c] Estimated from the GIAO MP2/tzp vs RHF/tzp correlation described in the text.

Lewis complexation also has a significant effect on the acetone carbonyl ^{13}C isotropic shift, e.g., 236.8 ppm for acetone·$AlCl_3$ at GIAO-MP2/qzp. Comparison of acetone·$AlCl_3$ and acetone·Al_2Cl_6 at RHF/qzp shows that the complex with the dimer has a much larger theoretical shift than the complex with the monomer; this is consistent with increased Lewis acidity, reflected in the structural differences noted in Figure 4.

Table 3 also reports calculated values of the principal components δ_{11}, δ_{22}, and δ_{33}; this information can also be cast as δ_{iso}, η, and CSA. The CSA values in Table 3 generally correlate with the size of the isotropic shifts. δ_{11} has the largest sensitivity to complexation with either a proton donor or an electron pair acceptor. Inspection of the data in Table 3 suggests no clear-cut criteria for distinguishing Brønsted and Lewis complexation on the basis of the acetone ^{13}C principal components. It is important to note that the GIAO-RHF isotropic chemical shift values are consistently greater than the GIAO-MP2 results, and the relationship between these values is a central theme of the following section.

Correlation between RHF and MP2 Shifts. Inspection of the data in Table 3 shows that there is a consistent relation between the GIAO-RHF and GIAO-MP2 isotropic chemical shifts over the range of compounds studied for either basis set scheme used. Linear regression of the data show that the GIAO-MP2/qzp shifts can be predicted with high accuracy from the GIAO-RHF/qzp calculations:

$$\delta_{MP2/qzp} = [1.12\ (\pm 0.04)]\delta_{RHF/qzp} - 42.1\ (\pm 10.5), \quad R^2 = 0.9974 \quad (2)$$

The numbers in parentheses in the preceding equation (and in those that follow) are the 95% confidence intervals. A plot of these data is shown in Figure 5. A similar relationship exists for the chemical shifts determined with the tzp/dz basis scheme, $\delta_{MP2/tzp} = [1.13\ (\pm 0.04)]\delta_{RHF/tzp} - 43.1\ (\pm 8.8)$, $R^2 = 0.9981$; however, we focus on the qzp data due to the higher quality of the basis sets and the better agreement with experimental values. Note that the difference between the GIAO-RHF/qzp and GIAO-MP2/qzp values is large, ranging from 7.8 ppm for protonated acetone to 14.7 ppm for acetone. This indicates that electron correlation has a significant influence on the chemical shifts. The high correlation coefficient indicates there is negligible error associated with the predictions.

We used this mathematical relationship to predict the GIAO-MP2/qzp shift of the acetone·zeolite complex and acetone·Al_2Cl_6 from the calculated GIAO-RHF/qzp values. For the acetone·zeolite complex, the predicted result is 225.6 ppm (cf. 223 ppm observed). For the acetone·Al_2Cl_6 molecule, the predicted value is 244.7 ppm (cf. 245 ppm observed). In both cases, the deviation from experiment for the GIAO-MP2/qzp results is 2.6 ppm or less, whereas the GIAO-MP2/tzp calculations disagree by as much as 4.5 ppm. In contrast, the GIAO-RHF/qzp calculations give predictions that disagree by as much

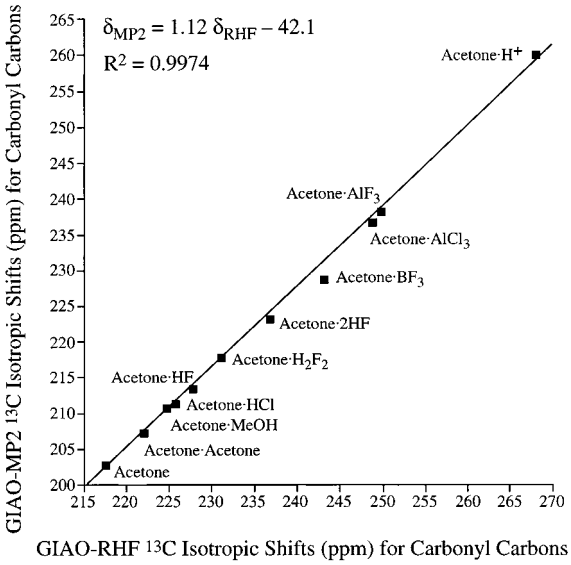

Figure 5. GIAO-MP2/qzp/tzp/dz vs GIAO-RHF/qzp/tzp/dz ^{13}C isotropic chemical shifts of the carbonyl carbon of acetone in various complexes. Data points are labeled with the chemical system they represent. The line represents the best least-squares fit line with the formula $\delta_{MP2} = [1.12\ (\pm 0.04)]\delta_{RHF} - 42.1\ (\pm 10.5)$ ppm ($R^2 = 0.9974$).

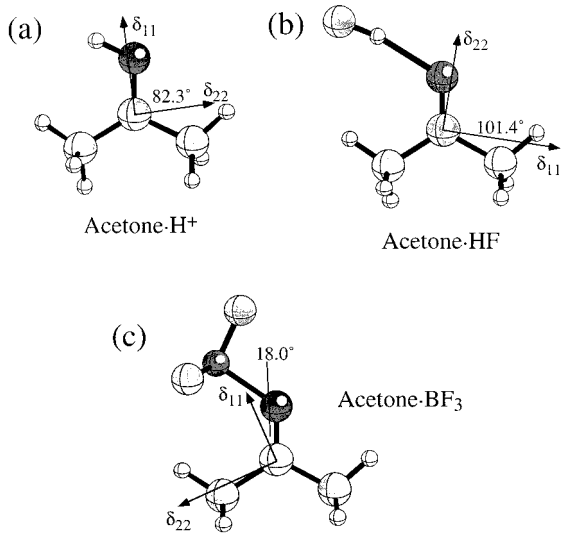

Figure 6. GIAO-MP2/qzp chemical shift tensor orientations for representative complexes: (a) δ_{33} lies 91.3° from the methyl carbon opposite the acidic proton; (b) δ_{33} leans 90.7° from the methyl carbon nearest HF; (c) δ_{33} lies within 1° of the perpendicular to the heavy atom plane.

as 15.4 ppm and the GIAO-RHF/tzp calculations overestimate the shift by as much as 10.5 ppm.

Even better agreement with experiment is obtained if we also correct for the difference between the calculated and measured isotropic shifts of gas-phase acetone. In this case, the theoretical value for the zeolite complex is 224.0 ppm (cf. 223 experimental) and that for acetone·Al_2Cl_6 is 243.1 ppm (cf. 245 experimental). Similarly good predictions of the chemical shifts for the zeolite and Al_2Cl_6 complexes are also obtained at the GIAO-MP2/tzp level if we adjust our theoretical results to the experimental value for gas-phase acetone. However, whereas similar adjustment of the GIAO-RHF results calculated with either basis set does give reasonable agreement for the zeolite complex (222.1 ppm), the adjusted GIAO-RHF value for the Al_2Cl_6 complex (239.1 ppm) is not sufficiently accurate to verify our theoretical model. This is, of course, due to the fact that the effects of correlation are not simply additive (the slopes of our regression equations are greater than 1) but increase as we move downfield. Thus, the GIAO-RHF calculations by themselves cannot be trusted to make accurate predictions.

Chemical Shift Tensors. One advantage to theoretical studies of chemical shift tensors is that the orientation of the tensor is provided by the calculation, whereas an experimental determination is very demanding and may not be possible. Figure 6 shows selected cases of the tensor orientations from the GIAO-MP2/qzp tensors plotted with the molecular geometry. We start with acetone. The C_2 symmetry of this molecule requires that one component lie along the C_2 rotation axis (the C−O bond); in this case, it is δ_{22}. The other two components lie in a plane perpendicular to the C−O bond; δ_{11} lies 0.4° out of the plane of the heavy atoms (leaning toward the H atom that is just out of the carbon plane), and δ_{33} lies 0.4° off the perpendicular to the carbon plane and is perpendicular to both δ_{11} and δ_{22}.

All but one of the complexes of acetone with a neutral proton donor have similar tensors for the carbonyl carbon: δ_{22} lies very near the C−O axis (typically less than 11.5°, but as much as 43.3° away); δ_{33} lies very nearly perpendicular to the carbon plane (as much as 0.7° away). For neutral proton donors, the δ_{22} component leans away from the proton donor molecule (on the other side of the carbonyl bond) when it is not exactly along the C−O bond. The exception is the acetone·2HF molecule, where δ_{11} (not δ_{22}) lies exactly (as required by symmetry) along the C−O bond. δ_{22} lies in the plane of the carbons, and δ_{33} is perpendicular to the carbon plane. For protonated acetone, δ_{11} (not δ_{22} as above) lies 7.7° off the C−O bond and it leans toward (not away from) the proton. δ_{22} lies 1.3° out of the carbon plane.

We now consider the complexes of acetone with Lewis acids. The complexes with AlF_3 and $AlCl_3$ have C_s symmetry. This requires that two of the components lie in the symmetry plane, and the other must be perpendicular to that plane. The perpendicular component in both cases is δ_{33}. δ_{11} is the component nearest the C−O bond, leaning toward AlF_3 and $AlCl_3$ in the complexes by 9.0 and 7.9°, respectively. δ_{22} is perpendicular to the other two components and lies on the same side of the carbonyl as the Lewis acid. The acetone·BF_3 complex has C_1 symmetry. As with the other Lewis acid models, δ_{11} is the component nearest the C−O bond, forming an angle of 18.0° with the carbonyl. δ_{22} lies 15.2° off of the C−C bond nearest the BF_3, and δ_{33} lies just 1° off the perpendicular.

Experimental ^{13}C Chemical Shifts. Measured ^{13}C chemical shift principal component data are reported in Table 4. Most notable from the standpoint of experimental challenge are the measurements made in frozen oleum (30% SO_3/H_2SO_4) and frozen SbF_5, for which isotropic shifts of 246 and 250 ppm, respectively, were determined. Hydrogen bonding has a large effect on the isotropic shift, and the value in $CF_3CH(OH)CF_3$ is almost as far downfield as that in zeolite HZSM-5. Table 4 confirms that δ_{11} is most strongly affected by complexation to an acid. δ_{22} and δ_{33} show little systematic dependence on acid strength.

Consistent with their theoretical counterparts, the experimental shifts are diagnostic of the strength but not type of acid complexed to acetone; the Brønsted and Lewis data are intercalated in Table 4. It is perhaps not surprising that the two classes of acids have similar effects on the acetone-*2*-^{13}C chemical shift tensor. The distinction between them is primarily

Table 4. Measured ^{13}C Chemical Shift Data for C-2 of Acetone in Various Acidic Media

system	temp, K	δ_{iso}, ppm	δ_{11}, ppm	δ_{22}, ppm	δ_{33}, ppm	CSA, ppm	η
CH_3COCH_3	77	210	288	265	77	−200	0.17
$CF_3CH(OH)CF_3$	77	221	309	276	78	−215	0.23
$MgCl_2$	77	221	319	267	77	−216	0.36
HZSM-5	93	223	314	269	86	−206	0.33
$MgBr_2$	77	223	327	262	80	−215	0.45
ZnI_2	77	227	325	274	83	−216	0.35
$ZnCl_2$	77	230	335	277	80	−225	0.39
$TaCl_5$	113	237	363	264	84	−230	0.65
AlI_3	77	238	375	266	73	−248	0.66
$ScTf_3$	113	239	370	262	86	−230	0.71
$AlBr_3$	77	243	396	265	69	−261	0.75
$AlCl_3$	193	245	387	256	93	−228	0.86
30% SO_3/H_2SO_4	77	246	392	280	66	−270	0.62
TaF_5	153	248	376	268	100	−222	0.73
SbF_5	77	250	404	280	67	−275	0.68

historical; Brønsted acids are just specific cases of electron-pair acceptors and are subsumed unto the general case of Lewis acids.

Discussion

The linear relationship between GIAO-MP2 isotropic ^{13}C shifts for the carbonyl of acetone and those at GIAO-RHF is an important and useful result. This relationship permits us to make accurate estimates of chemical shifts for acetone in theoretical structures that more realistically model adsorption sites than those which can be explicitly treated with actual GIAO-MP2 shift calculations. We do not expect the equation in Figure 5 to be directly applicable to other molecules in acidic media, even other ketones or aldehydes, because the effect of electron correlation on chemical shift will necessarily vary from molecule to molecule. In particular, for acetone the change in chemical shift over the range of molecules studied is highly correlated to the change in the length of the carbonyl double bond. The fact that the inclusion of electron correlation has a well-behaved effect on the chemical shift for a series of molecules with slight variations in geometry is not surprising. Our limited experience with calculations of complexes of other basic adsorbates with acids suggests that useful correlations such as that in Figure 5 may also apply.

There has been a previous study of acetone and protonated acetone with the LORG method without correlation.[47] The earlier workers obtained isotropic chemical shifts of 207.9 ppm for acetone and 243.9 ppm for protonated acetone. As noted above, we obtain 202.8 and 260.1 ppm for the same molecules. Given that the gas-phase chemical shift for acetone is 201.2 ppm, the GIAO-MP2 result is in better agreement with experiment. The experimental chemical shift for acetone in highly acidic media, in which we expect full protonation, is in the range 246−250 ppm. In this case, the LORG prediction is in much closer agreement with the experimental values. It is not clear that the experimental values for protonated acetone in solution should be accurately represented by a theoretical calculation that corresponds to an isolated, gas-phase molecule and ignores the anion and solvent. In a combined theoretical and experimental study of the isopropyl cation, we also observed that the MP2 shift was downfield of the experimental values in SbF_5, but inclusion of anions, FHF^- or SbF_5^-, substantially improved agreement. We believe that similar effects account for the shifts in protonated acetone.

We have focused on the correlation for δ_{iso} because the isotropic chemical shift is generally the most accurate when compared to experiment and it is the most common experimentally determined NMR observable. We have, however, also found an analogous correlation for the CSA: $CSA_{MP2/qzp} = [1.15\ (\pm 0.05)]CSA_{RHF/qzp} - 77.0\ (\pm 12.5)$ ppm, $R^2 = 0.9967$. Unfortunately, the correlation of η_{MP2} vs η_{RHF} shows more scatter: $\eta_{MP2/qzp} = [0.956\ (\pm 0.29)]\eta_{RHF/qzp} - 0.0\ (\pm 0.1)$ ppm, $R^2 = 0.8682$. The same analysis of the tzp/dz data yields $CSA_{MP2/tzp} = [1.16\ (\pm 0.04)]CSA_{RHF/tzp} - 75.0\ (\pm 8.7)$ ppm, $R^2 = 0.9984$ and $\eta_{MP2/tzp} = [0.967\ (\pm 0.26)]\eta_{RHF/tzp} - 0.01\ (\pm 0.10)$ ppm, $R^2 = 0.8926$. For completeness, we have included plots analogous to the one in Figure 5 for $\delta_{iso/tzp}$ as well as CSA and η with both the qzp and tzp data in the Supporting Information.

We are very satisfied with the agreement between experimental isotropic shifts and the estimated GIAO-MP2/qzp shifts. In the case of the acetone·zeolite cluster, the best predicted value is 224.0 ppm, which is in very good agreement with our experimental value of 223 ppm for zeolite HZSM-5. This agreement supports our interpretation of Figure 1 as a quantitative depiction of the equilibrium geometry of acetone on a zeolite Brønsted site. While we necessarily expect that the application of even higher levels of theory to the model in Figure 1, or the use of larger clusters to approximate the zeolite, will result in modest changes in bond distances or angles, the essential features of Figure 1 will not be altered.

For the acetone·Al_2Cl_6 complex, the predicted GIAO-MP2/qzp shift of 243.1 ppm is in very good agreement with the experimental value of 245 ppm. It is clear that Al_2Cl_6 is a much better model for adsorption on aluminum chloride powder than the $AlCl_3$ monomer. The structures of complexes with metal halide powders are not as well characterized as those on zeolites, which have well-known framework structures. Given the lack of atomic-level experimental information about metal halide adsorption complexes, further theoretical modeling would seem premature. We are satisfied with the present agreement obtained for acetone·Al_2Cl_6.

In retrospect, we could have used only the GIAO-MP2/tzp level of theory, with adjustment of the theoretical values to the experimental gas-phase acetone chemical shift. As was demonstrated, the use of an internal reference clearly corrects for deficiencies in the basis set. In addition, such adjustment also approximately corrects for errors that may arise due to our limited correlation treatment and neglect of vibrational effects. Still, the demonstration that the larger basis set gives better agreement with experimental values should serve as a useful guideline for future work.

Conclusion

We have made the important and useful discovery of a linear relationship between GIAO-MP2 and GIAO-RHF ^{13}C isotropic shifts for acetone in various complexes with either proton donors or electron pair acceptors. This relationship, determined exclusively from theoretical data, allows us for the first time to make reliable estimates of ^{13}C chemical shifts for an adsorbate (acetone) complexed to cluster models sufficiently large to approximate the properties of zeolite solid acids and metal halide powders. The excellent agreement between the experimental ^{13}C isotropic shift of acetone adsorbed on zeolites and the predicted GIAO-MP2/qzp result for our theoretical model is evidence in support of the quantitative accuracy of this structure.

Acknowledgment. Work at Texas A&M University was supported by the National Science Foundation (Grant CHE-9528959), the U.S. Department of Energy (DOE) (Grant DE-

FG03-93ER14354), and the Robert A. Welch Foundation. J.B.N. was supported by the Office of Basic Energy Sciences of DOE and by Laboratory Directed Research and Development funding provided by Pacific Northwest National Laboratory (PNNL). Computer resources at Texas A&M were provided by the Texas A&M University Supercomputing Facility. Computer resources were also provided by the Scientific Computing Staff, Office of Energy Research, at the National Energy Research Supercomputer Center (NERSC), Livermore, CA. PNNL is a multiprogram national laboratory operated by Battelle Memorial Institute for DOE under Contract DE-AC06-76RLO1830.

Supporting Information Available: Figures showing the optimized geometries of acetone·HCl and acetone·AlF_3 and plots of GIAO−MP2 vs GIAO-RHF data for qzp/tzp/dz (CSA and η) and tzp/dz (δ_{iso}, CSA, and η) basis set schemes (6 pages, print/PDF).

JA982226W